Muscle and Nerve

THE ADAPTIVE RESPONSES OF TRPC1 AND TRPC3 DURING SKELETAL MUSCLE ATROPHY AND REGROWTH

Journal:	*Muscle and Nerve*
Manuscript ID:	
Wiley - Manuscript type:	Research Article
Date Submitted by the Author:	n/a
Complete List of Authors:	Zhang, Bao-Ting; Hong Kong Polytechnic University, Department of Rehabilitation Sciences Yeung, Simon; Hong Kong Polytechnic University, Department of Rehabilitation Sciences Cheung, Kwok-Kuen; Hong Kong Polytechnic University, Department of Rehabilitation Sciences Chai, Zacary; Hong Kong Polytechnic University, Department of Rehabilitation Sciences Yeung, Ella; Hong Kong Polytechnic University, Department of Rehabilitation Sciences
Keywords:	TRPC1, TRPC3, muscle atrophy, muscle regeneration, hindlimb suspension

THE ADAPTIVE RESPONSES OF TRPC1 AND TRPC3 DURING SKELETAL MUSCLE ATROPHY AND REGROWTH

BAO-TING ZHANG, MD,[1,2] SIMON S. YEUNG, PhD,[1] KWOK-KUEN CHEUNG, PhD,[1] ZACARY Y. CHAI, BSc,[1] ELLA W. YEUNG, PhD[1*]

[1]Muscle Physiology Laboratory, Department of Rehabilitation Sciences, The Hong Kong Polytechnic University, Hung Hom, Kowloon, Hong Kong

[2] Current address: School of Chinese Medicine, The Chinese University of Hong Kong, Hong Kong

[*] **Correspondence to:** Ella W. Yeung; e-mail: ella.yeung@polyu.edu.hk

Acknowledgements: The authors gratefully acknowledge support of this work by the Hong Kong Research Grants Council General Research Fund (PolyU 5635/12M to EWY) and the Hong Kong Polytechnic University Central Research Grant (G-YL11 to EWY).

Running title: Adaptive response of TRPC1 and TRPC3

ABSTRACT

Introduction: We assessed the time-dependent changes of transient receptor potential channel 1 (TRPC1) and TRPC3 expression and localization associated with muscle atrophy and regrowth *in vivo*.

Methods: Mice were subjected to hindlimb unloading for 7 or 14 days (7U, 14U), followed by 3, 7, or 14 days of reloading (3R, 7R, 14R).

Results: Soleus muscle mass and tetanic force were reduced significantly at 7U and 14U and recovered by 14R. Recovery of muscle fiber cross-sectional area was observed by 28R. TRPC1 mRNA was unaltered during the unloading-reloading period. However, protein expression remained depressed through 14R. Decreased localization of TRPC1 to the sarcolemma was observed. TRPC3 mRNA and protein expression levels were decreased significantly during the early phase of reloading.

Discussion: Given the known role of these channels in muscle development, changes observed in TRPC1 and TRPC3 may relate closely to the muscle atrophy and remodeling processes.

Keywords: TRPC1; TRPC3; muscle atrophy; muscle regeneration; hindlimb suspension

INTRODUCTION

Skeletal muscles exhibit high plasticity in response to mechanical load. Muscle growth and maintenance processes are regulated by intracellular signaling cascades that control transcription and protein translation. Rodents subjected to mechanical unloading demonstrated a decrease in muscle mass, myofiber cross-sectional area (CSA), and force generation. Subsequent reloading triggers a cascade of events involving mild muscle injury, inflammation, regeneration, and growth that results in recovery of muscle mass and CSA.[1,2] A hallmark of muscle regeneration is activation of satellite cells committed to myogenesis and induction of myogenic regulatory factors.[3] A more complete understanding of the mechanisms involved in muscle atrophy and regeneration will aid in development of new therapies for conditions and diseases such as muscular dystrophy, disuse atrophy, and aging.

The effects of mechanical unloading/reloading on expression levels of muscle-specific transcription factors and proteins are time-dependent. Multiple catabolic and anabolic signaling pathways are associated with alterations of muscle size.[4-6] Evidence has accumulated that the size of the muscle is determined by a balance between protein synthesis and protein degradation.[5] Findings suggest that calcium Ca^{2+}-dependent signaling pathways play a role in mediating both atrophic and regrowth processes during unloading and reloading, respectively.[7-9] Evidence has shown an increase in intracellular Ca^{2+} ($[Ca^{2+}]_i$) concentration as early as the second day of unloading.[7,10] Such an increase would promote Ca^{2+}-dependent proteolysis leading to significant degradation of cytoskeletal proteins.[11] Muscle regrowth after a period of disuse involves both muscle hypertrophy and regeneration, where muscle regeneration is characterized by myoblast proliferation and differentiation as well as upregulation of muscle regulatory factors.[12,13] A key role for Ca^{2+} entry in myogenic commitment, differentiation, and myotube fusion is well recognized.[14,15]

Transient receptor potential canonical (TRPC) channels, particularly TRPC1 and TRPC3 isoforms, are expressed abundantly in adult skeletal muscle fibers. These Ca^{2+}-permeable non-selective channels have been shown to be associated with muscle growth and development. TRPC1 is known to mediate Ca^{2+} entry, thereby regulating myoblast migration and differentiation.[16,17] Previous work has also demonstrated a role for TRPC1 during muscle regeneration by modulating the PI3K/Akt pathway.[18] TRPC3, another TRPC family protein, is highly expressed in skeletal muscle.[19,20] We[21] and others[22] have reported that TRPC3 is upregulated in the early phase of myotube differentiation. Furthermore, it has been suggested that TRPC3 mediates Ca^{2+} influx leading to downstream activation of nuclear factor of activated T cells (NFAT) in skeletal muscle remodeling.[23] The aim of this study, therefore, was to determine how mechanical perturbations impact time-dependent TRPC1 and TRPC3 expression in mouse soleus muscle. We hypothesize that TRPC1 and TRPC3 levels are related closely to the amount of muscle atrophy and regrowth observed during 14 days of hindlimb unloading and 14 days of reloading, respectively.

MATERIALS and METHODS

Ethics Statement

All animal handling procedures and experimental protocols were approved by the Animal Ethics Committee of the Hong Kong Polytechnic University (ASESC no. 07/24).

Animals

Male BALB/c mice (8-10 weeks old) were housed in a temperature-controlled facility with a 12-hour light/dark cycle and had *ad libitum* access to food and water. The animals were allowed to acclimatize for at least 7 days before beginning the experiments.

Group allocation

Animals were randomized into 1 of the following experimental groups (n = 5 in each group): hindlimb unloaded for 7 days (7U) or 14 days (14U); hindlimb unloaded for 14 days followed by reloading for 3 days (3R), 7 days (7R), or 14 days (14R). In some experiments, 28 days of reloading (28R) was performed when the measured parameters did not return to control levels. For each experimental group, weight-bearing, age-matched controls were included (n = 5 in each control group).The body weight of the mice was measured weekly from the start of the experiment.

Hindlimb unloading and reloading procedure

The hindlimb unloading procedure was performed as described previously.[24] Briefly, orthopedic adhesive tape was applied to the proximal one-third of the tail and placed through a metal ring that attached to a metal bar on the top of a hindlimb suspension cage. The suspension height was adjusted to maintain a suspension angle of 30° to ensure that the hindlimbs were unable to touch any supporting surface. The forelimbs were allowed contact with the gridded bottom of the cage so that the animals could move and freely access food and water. For the reloading groups, the animals were released from suspension after 14 days and allowed to resume normal weight bearing.

Muscle wet mass and force measurements

At designated time points, the mice were sacrificed *via* cervical dislocation. The soleus muscles were isolated and weighed. The muscle wet mass values were normalized to body weight, and the data are expressed as mg/g body weight.

Dissected muscle tissue was bathed in Krebs solution (in mM): NaCl 121, KCl 5, $CaCl_2$ 1.8, $MgCl_2$ 0.5, NaH_2PO_4 0.4, $NaHCO_3$ 24, and glucose 5.5 (bubbled with 95 % O_2 - 5 % CO_2, pH 7.4 at 24 °C) for force testing as described previously.[25] Briefly, the proximal and distal tendons of the muscles were gripped with T-shaped aluminum foil clips. One end of the tendon was attached to a hook connected to the lever arm of a position feedback motor (300B-LC, Aurora Scientific, Aurora, Canada), and the other end was attached to a force transducer (Model BG-10, Kulite Semiconductor Products Inc., Leonia, NJ). The force transducer was clamped to a mechanical micromanipulator for adjustment of muscle length. The muscle was stimulated with 0.5 ms pulses of supramaximal intensity. Peak isometric tetanic force (P_o) was obtained by stimulating (S48, Grass Technologies, West Warwick, RI) the muscle at 100 Hz for a train duration of 400 ms at optimum length. P_o was normalized to whole muscle cross-sectional area.

Histology

Isolated soleus muscles were frozen immediately in liquid nitrogen-chilled isopentane and cryoembedded with OCT (Metronet Technology Ltd., Hong Kong, China) for sectioning. Cross sections (6 µm thick) were cut from the midbelly of the muscle. Sections were fixed in 4% paraformaldehyde in phosphate-buffered saline (PBS, pH 7.4), rinsed, and stained with hematoxylin and eosin solution followed by dehydration and mounting. Sections were visualized using a light microscope, and images of a muscle sections (4× objective magnification) were captured using a Spot camera (Carl Zeiss MicroImaging, Inc., Jena, Germany). The total muscle area and the total number of fibers were determined using Image J software (National Institutes of Health, Bethesda, MD). Muscle fiber cross-sectional area (CSA) was obtained by dividing the area of the entire muscle cross-section by the fiber number and is expressed in μm^2.

Real-time PCR

Total RNA of soleus muscles was extracted using the SV total RNA isolation system (Promega, Madison, WI), and cDNA was synthesized from 0.5 µg total RNA of each soleus sample using a SuperScript III First-Strand Synthesis Kit (Invitrogen, Carlsbad, CA) according to manufacturer instructions. TaqMan® gene expression assay with primers and minor groove binder (MGB) probes that were specific for murine TRPC1 and TRPC3 (Assay ID: Mm00441975 for TRPC1 and Mm00444690 for TRPC3; Applied Biosystems, Foster City, CA) were used for real-time PCR. The amplification was performed in a 7500 real-time PCR system (Applied Biosystems) as described previously.[21] GAPDH was used as an endogenous control for normalization. Each sample was assessed in triplicate. Relative changes in TRPC1 and TRPC3 receptor gene expression were determined using the $2^{-\Delta\Delta Ct}$ (normalized expression ratio) method of analysis.[26]

Western blot analysis

Soleus muscles were collected for Western blot analysis as described previously[21] with minor modifications. Briefly, the soleus muscles were homogenized on ice in 1× RIPA buffer (Cell Signaling Technology, Beverly, MA) containing protease inhibitor cocktail (Roche , Mannheim, Germany) and 1 mM PMSF (Merck, Darmstadt, Germany). After centrifugation, the extracted protein was quantified using the Bradford Assay (Quick Start Bradford Protein Assay Kit, Bio-Rad, Hercules, CA). Forty-five µg of protein were separated by SDS-PAGE and transferred onto nitrocellulose membranes (Perkin Elmer, Waltham, MA). After blocking with 5% nonfat dry milk (Bio-Rad) in Tris buffered saline (TBS) containing 0.05 % Tween 20, the membranes were probed with primary antibodies and subsequently with Near Infrared dye-conjugated secondary IgG (LI-COR Biosciences, Lincoln, NE). Immunoreactive bands

were detected using the Odyssey® Infrared Imaging System (LI-COR) and quantified using a 1-D image analysis system (LI-COR). The primary antibodies used were monoclonal antibody against TRPC1 and GAPDH (Santa Cruz Biotechnology, Santa Cruz, CA) and a polyclonal antibody against TRPC3 (Alomone Labs, Jerusalem, Israel). Expression of TRPC1 and TRPC3 was calculated by first normalizing the band intensity to GAPDH as control. The GAPDH normalized expression of proteins from the experimental groups was represented as a percentage of GAPDH normalized age-matched controls. The value was thus expressed as the percentage of the age-matched control level.

Fluorescence immunohistochemistry

Muscle sections were fixed in pre-cooled acetone at 4 °C and permeabilized using 0.2 % Triton X-100. Non-specific binding was blocked using 5% normal horse serum. Sections were incubated with primary antibodies targeting TRPC1 (1:80; Santa Cruz Biotechnology) and TRPC3 (1:80; Alomone Labs) receptors separately, followed by Alexa Fluor 488-conjugated secondary antibodies (Invitrogen). For TPRC1, 2 rabbit polyclonal anti-TRPC1 antibodies (1:50, Santa Cruz Biotechnology; 1:200, Alomone Labs) were used to confirm the immunoreactive pattern. Anti-TRPC1 antibody was preadsorbed by incubating the antibody with its blocking peptide serving as a negative control.

For sarcolemmal localization, TRPC1 immunostained muscle sections were incubated with TRITC-conjugated wheat germ agglutinin (TRITC-WGA, 1: 500; Molecular Probes) for 1 h at room temperature. The washed sections were mounted with DAPI-containing Vectorshield (Vector Labs, Burlingame, CA) for nuclei identification. The images were visualized with a fluorescence microscope (40× objective, Eclipse 80i; Nikon, Tokyo, Japan) and were captured using the Spot-advanced software.

Statistics

Differences in muscle mass, fiber CSA, force, and mRNA and protein expression of TRPC1 and TRPC3 at each time point were compared to their corresponding age-matched control groups by unpaired *t*-tests. To examine the differences between experimental groups over the time course of the unloading-reloading period, one-way ANOVA and Bonferroni *post-hoc* multiple comparison tests were used to examine all parameters. Pearson correlation coefficients were calculated between fiber CSA, TRPC1, and TRPC3 under control conditions and across all days of unloading and reloading. Values are presented as means ± SEM. $P < 0.05$ was considered statistically significant.

RESULTS

We investigated the cellular and molecular events that occur during muscle atrophy and regrowth. We focus on TRPC1 and TRPC3 because of their known regulatory roles in muscle development and function.

Body weight

At each time point of this study, the body weight of the animals in each experimental group was compared to that of age-matched controls (Table 1). No significant differences were observed at any time.

Soleus muscle mass

At days 7 and 14 of hindlimb suspension, the soleus muscle mass decreased to 74 ± 10% and 62 ± 4%, respectively, of age-matched control levels ($P < 0.05$ for both) and remained decreased after 3 and 7 days of reloading (3R: 68 ± 9%, 7R: 76 ± 4% with respect to

age-matched controls, $P < 0.05$). After 14 days of reloading, muscle mass was normalized to that observed in age-matched control soleus muscles (14R: 103 ± 14 %).

Figure 1 shows the muscle mass to body weight ratio at different periods of the experiment. There was a significant change over time ($P < 0.001$, ANOVA). Similar to muscle mass, this ratio was significantly lower in 7U and 14U ($P < 0.01$), 3R and 7R ($P < 0.05$) compared to controls. At 14U, the decrease was ~0.60-fold compared to 14R ($P < 0.01$). The muscle mass to body weight ratio was fully restored to control values in 14R.

Muscle fiber cross-sectional area

Changes in the mean soleus muscle fiber CSA during the experiment are shown in Figure 2. A significant change in CSA was observed ($P < 0.0001$, ANOVA). Following 7U and 14U, fiber CSA was reduced significantly to 63 ± 3 % and 43 ± 2 %, respectively, compared to controls. Although subsequent reloading for 3, 7, and 14 days led to gradual recovery, the mean CSA was significantly smaller than the CSA observed in controls at these time points (3R: 48 ± 2 %; 7R: 56 ± 2 %; 14R: 74 ± 4 %; all $P < 0.001$). The fiber CSA did not return to control levels until after 28 days of reloading.

Peak tetanic force

Figure 3 shows changes in P_o during the experimental period. P_o declined significantly to 66 ± 8 % and 57 ± 5 % of age-matched controls following 7U and 14U, respectively ($P < 0.01$ for both). After 3 days of reloading, P_o only recovered to approximately 63% of controls ($P < 0.01$). P_o recovered to the levels of the age-matched controls (101 ± 10%) after 14R.

TRPC1 and TRPC3 mRNA expression

The transcript expression of TRPC1 and TRPC3 for soleus muscle relative to GAPDH was assessed by real-time PCR. There was no change in GAPDH expression during unloading and reloading. TRPC1 and TRPC3 mRNA transcript expression at each time point did not differ from age-matched controls. Although the levels of TRPC1 mRNA appeared to be lower after 7U (Fig. 4A), there was no significant change over the course of unloading and reloading.

A significant difference in TRPC3 mRNA was observed during the experiment ($P < 0.01$, ANOVA). Although no change was observed in TRPC3 mRNA at 7 days or 14 days unloading, TRPC3 mRNA levels were lower than those for controls after 3 days of reloading ($P < 0.05$). At 3R and 7R, TRCP3 mRNA levels were decreased significantly relative to 14R (3R: $P < 0.01$; 7R: $P < 0.05$) (Fig. 4B).

TRPC1 and TRPC3 protein expression

TRPC1 and TRPC3 protein expression following unloading and reloading was detected by Western blotting (Fig. 5). There was no change with GAPDH expression. TRPC1 expression decreased significantly to 85 ± 4 % and 78 ± 5 % of age-matched control levels after 7U and 14U, respectively (*vs*. age-matched control, both $P < 0.05$).

TRPC1 protein expression during the experimental period was also decreased (Fig. 5A, $P < 0.001$, ANOVA). Unloading for 14 days led to a significant decrease in the TRPC1 expression level ($P < 0.05$). During reloading, the expression remained lower after 3 days, 7 days, and even after 14 days (3R: 68 ± 4 %; 7R: 61 ± 3 %; 14R: 78 ± 4 %, all $P < 0.01$). Expression returned to control levels after 28 days of reloading (106 ± 6%).

TRPC3 protein expression varied significantly over the time course of the experiment (Fig. 5B). TRPC3 expression decreased to 87 ± 4 % of age-matched control levels following

14 days of unloading. At 3R, the expression of TRPC3 was still significantly lower compared to control but completely recovered by 14R (98 ± 3%).

Correlation between unloading-reloading associated changes in TRPC1, TRPC3 and fiber CSA

A significant correlation between fiber CSA and TRPC1 protein expression was observed in 7U ($R^2 = 0.89$; $P < 0.001$) and 14U ($R^2 = 0.85$; $P < 0.001$). In addition, there was a strong trend between fiber CSA and TRPC3 protein expression, but this relationship failed to reach significance ($R^2 = 0.63$; $P = 0.055$). During the early period of reloading (3R, 7R), neither TRPC1 nor TRPC3 expression was correlated with fiber CSA. During this period the protein expression levels remained depressed, while significant increases in fiber CSA were observed.

Immunohistochemistry of TRPC1 and TRPC3

The staining pattern of TRPC1immunohistochemistry obtained from cross-sections was examined. TRPC1-dependent immunoreactivity co-localized with TRITC-WGA and was localized predominantly to the sarcolemma region (Fig. 6A). Minor punctate staining for TRPC1 in sarcoplasm was also observed. TRPC1 immunoreactivity was downregulated dramatically after 14U. The expression in the sarcolemma was reduced substantially; the punctate staining disappeared in the sarcoplasm. By 14R, an increase in TRPC1 expression in the sarcolemma was observed. However, TRPC1-dependent staining in the sarcoplasm was still absent. After 28 days of reloading, the strong sarcomlemmal TRPC1 staining observed in control muscles was restored, and the punctate staining of TRPC1 in the sarcoplasm was again detected. Similar results were obtained using another antibody source indicating TRPC1-specificity of the observed staining.

The TRPC3-dependent immunostaining pattern was distinctly different from that of TRPC1 (Fig. 6B). TRPC3 was expressed in the sarcolemma as well as within the myofibers. Furthermore, the expression of TRPC3 was checkerboard-like, with some myofibers showing stronger immunoreactivity than others. The expression of TRPC3 at 14U was reduced, but the staining intensity was restored after 7 days of reloading.

DISCUSSION

TRPC1 and TRPC3 have been implicated in many pathophysiological processes in skeletal muscle related to muscle development, Ca^{2+} signaling, and Ca^{2+} homeostasis.[27] Therefore, the purpose of this study was to examine time-dependent changes in TRPC1 and TRPC3 expression in mouse soleus muscles during mechanical unloading and reloading.

The time-dependent unloading-reloading changes in the contractile properties of the soleus muscle reported here were similar to those observed in other studies.[28,29] The soleus muscle mass normalized to body weight was reduced significantly after unloading relative to that of age-matched controls. These data imply that reduction of muscle mass was due to the removal of mechanical stress. A significant loss in muscle mass and P_o was observed after 7 or 14 days of unloading, but both parameters recovered fully to their control values after 14 days of reloading. Interestingly, the time for recovery of fiber CSA took longer. After 14 days of reloading, fiber CSA was only 72% of that in the control group. This finding is consistent with other studies[30] and suggests that the recovery of atrophic muscle fibers involves not only growth but also regeneration. Thus, recovery of the CSA of atrophic fibers continues after increases of muscle mass. Recovery of muscle mass is normally complete after 14 days of reloading even if the unloading period extends beyond 10 days, whereas processes related to complete regeneration, such as CSA recovery, can extend up to 5 weeks.[30,31]

In the soleus, TRPC1 is the most abundantly expressed TRPC isoform.[20] We found a significant decrease of TRPC1 protein expression after 14 days of unloading even though the mRNA level had not changed. Changes in mRNA level may not necessarily reflect that of the proteins in catabolic muscle, where there is suppressed protein synthesis and increased protein degradation.[32] Reduced TPRC1 protein expression (~78%) was not restored to control values even after 14 days of reloading, suggesting that TRPC1 protein expression is regulated at the post-transcriptional level.

The localization of TRPC1 at the sarcolemma, together with its assembly in a Ca^{2+} channel complex, is key to its function and regulation.[33] Localization of TRPC1 to the sarcolemma was greatly diminished upon unloading but returned to control levels after reloading. However, the depressed expression lagged behind recovery of the contractile function. Although the immunostaining data were not objectively quantified, downregulation of TRPC1 expression in the sarcolemma was more extensive and implies its known functional role. The punctate cytoplasmic staining observed may represent the distribution of TRPC1 in the endoplasmic reticulum (ER) or endosomal compartments. Interestingly, the punctate staining disappeared after 14 days of unloading. Whether the recycling of TRPC1 depends on other mechanosensitive mechanisms requires further investigation.

It is unclear whether TRPC1 modulation is mediated directly by a mechanical stimulus or if it is part of a larger signaling pathway. There are 2 possible causes for downregulation of TRPC1 during unloading. The first possibility is that TRPC1 plays a role in mechanically-induced signal transduction in muscles and becomes downregulated when mechanical stress is removed, such as the unloading here. Skeletal muscle growth and development is dictated by the amount of mechanical load imposed. Removal of mechanical stress has been shown to decrease the mechanical properties of the muscle.[34,35] TRPC1 channels have been implicated in mediating Ca^{2+} entry in skeletal myoblast migration and

differentiation.[17] Expression of TRPC1 is upregulated markedly during myogenesis in the presence of sphingosine 1-phosphate,[16] a pro-myogenic molecule involved in satellite cell proliferation and muscle regeneration.[36,37] TRPC1-siRNA treatment reduced store-operated Ca^{2+} entry (SOCE), reduced the expression of myogenic differentiation markers, and subsequently suppressed skeletal myogenesis.[16] It was recently reported that the level of TRPC1 expression correlates with the magnitude of SOCE.[38] Therefore, the decreased TRPC1 expression observed here may lead to a reduction in SOCE, thereby affecting key steps in myogenesis. This loss of TRPC1 may also account for the our results[24,39] and those of others[40,41] that show hindlimb unloading suppresses satellite cell proliferation and differentiation.

The second possible explanation for the decrease in TRPC1 expression during unloading is a negative feedback mechanism that serves to limit $[Ca^{2+}]_i$ elevation. Disrupted intracellular Ca^{2+} signaling is involved in muscle atrophy. Many studies support the assertion that $[Ca^{2+}]_i$ is increased in unloaded soleus muscles.[7-9] This increase in $[Ca^{2+}]_i$ may be related to cytoskeletal network disruption causing an increase in sarcolemmal permeability for Ca^{2+}, or more likely activation of the Ca^{2+}-activated protease calpain.[42-45] Furthermore, Singh et al.[46] demonstrated that overexpression of calmodulin led to a reduction in TRPC1-related SOCE, which was achieved *via* calmodulin interaction with a domain in the C terminus of TRPC1. Therefore, the expression and activity of theTRPC1 may be part of a negative feedback mechanism poised to respond to increased $[Ca^{2+}]_i$ levels.[47]

Decreased TRPC1 expression persisted for 14 days after reloading. The physiological role of TRPC1 downregulation remains unclear, but it is well known that reloading after disuse involves muscle regeneration and growth processes.[30] Two signaling pathways, namely the Akt/ PKB and calcineurin (CaN) pathways, play an important role in this regulation. A role for TRPC1 channels in modulating PI3K/Akt pathway during muscle

regeneration was reported recently.[18] In a cardiotoxin-induced muscle injury model, mice lacking TRPC1 exhibited delayed regeneration accompanied by decreased expression of myogenic factors (MyoD, Myf5 and myogenin) and reduced Akt phosphorylation, demonstrating an essential role of TRPC1 in muscle regeneration.

CaN-NFAT signaling is a Ca^{2+}-dependent pathway. Several studies[31,48] of time-dependent changes in signal transduction pathways involved in muscle regrowth have shown that CaN signaling is not involved in the early stages of reloading but only become elevated at later stages of muscle remodeling. Specifically, Sugiura et al.[48] examined a 10-day hindlimb unloading period and showed that CaN levels in muscle were not elevated until 10 days after reloading. Furthermore, Oishi et al.[49] showed that recovery of fiber size after reloading was inhibited in rats that were treated with a CaN inhibitor. In a functional study Pigozzi et al.[50] reported that upregulation of TRPC1 (and TRPC3) involves activation of the Ca^{2+}-CaN-NFAT cascade. The authors demonstrated that thapsigargin-induced overexpression of TRPC1 (and TRPC3) was diminished in the presence of a CaN inhibitor. They also showed that the induction of TPRC1 (and TRPC3) led to translocation of NFAT to the nucleus. It is therefore possible that the upregulation of TRPC1 observed at the later stage of reloading may parallel the timing of increased CaN levels and participate in recovery of muscle fiber size. The participation of TRPC1 expression and associated Ca^{2+} entry in CaN-dependent muscle remodeling warrants further investigation.

TRPC3 has been implicated in mediating myogenic tone in arteries,[51] but the channel is not gated mechanically. A possible role of TRPC3 in muscle atrophy and regrowth could be through its ability to regulate muscle cell differentiation.[21,22] TRPC3 expression is upregulated in myotube differentiation and is functionally coupled to RyR1. Here, we observe no changes in TRPC3 at the transcriptional level during unloading, but both mRNA and protein expression levels were decreased significantly during the early phase of

reloading. However, TRPC3 expression was restored to baseline levels upon 14 d of mechanical reloading. The immunostaining pattern of TRPC3 was mainly intracellular. The physiological relevance of this localization pattern requires further investigation.

TRPC3 has been demonstrated to be involved in NFAT activation in response to exercise, suggesting that increased expression of TRPC3 mediated the rise in $[Ca^{2+}]_i$ responsible for regulation of CaN-NFAT signaling.[23] Taken together with the observations of Pigozzi et al.[50] described earlier, it is possible that TRPC3 forms a positive regulatory circuit with the CaN-NFAT pathway during the later stage of muscle regeneration upon reloading. TRPC3 gene transcription could be activated by the CaN-NFAT pathway with an increase in the expression of TRPC3 further activating the CaN-NFAT pathway. In fact, a regulatory signaling circuit of TRPC6-CaN-NFAT that coordinates cardiac hypertrophy and remodeling in response to mechanical stress has been reported.[52]

This study shows that 14 days of mechanical unloading led to significant loss in soleus muscle mass and force. Impaired recovery during early reloading was observed, but it improved in a time-dependent manner. TRPC1 and TRPC3 responded differently to mechanical perturbation *in vivo*. Both TRPC1 and TRPC3 protein expression was reduced at 14 days of unloading, with TRPC1 being affected more. Of interest, expression of both TRPC1 and TRPC3 showed a significant decrease during the early stages of reloading, and the recovery of TRPC1 expression required more time. The interplay between Ca^{2+}-sensitive signaling molecules (such as CaN) and TRPC1 and/or TRPC3 may contribute to the activation of a Ca^{2+}-dependent signaling pathway leading to muscle remodeling and regrowth.

Abbreviations:

7U, or 14U, 7 or 14 days of hindlimb unloading; 3R, 7R or14R, 3, 7, or 14 days of reloading; Ca^{2+}, calcium ions; CaN, calcineurin; $[Ca^{2+}]_i$, intracellular Ca^{2+}; CSA, cross-sectional area; NFAT, nuclear factor of activated T cells; P_o, peak isometric tetanic force; PI3K-Akt, phosphatidylinositol 3'-kinase; SOCE, store-operated Ca^{2+} entry, TRPC1: transient receptor potential canonical type 1;TRPC3: transient receptor potential canonical type 3.

REFERENCES

1. Adams GR, Caiozzo VJ, Baldwin KM. Skeletal muscle unweighting: spaceflight and ground-based models. J Appl Physiol 2003;95:2185-2201.

2. Fitts RH, Riley DR, Widrick JJ. Physiology of a microgravity environment invited review: microgravity and skeletal muscle. J Appl Physiol 2000;89:823-839.

3. Charge SB, Rudnicki MA. Cellular and molecular regulation of muscle regeneration. Physiol Rev 2004;84:209-238.

4. Chopard A, Hillock S, Jasmin BJ. Molecular events and signalling pathways involved in skeletal muscle disuse-induced atrophy and the impact of countermeasures. J Cell Mol Med 2009;13:3032-3050.

5. Glass DJ. Signalling pathways that mediate skeletal muscle hypertrophy and atrophy. Nat Cell Biol 2003;5:87-90.

6. Rennie MJ, Wackerhage H, Spangenburg EE, Booth FW. Control of the size of the human muscle mass. Annu Rev Physiol 2004;66:799-828.

7. Ingalls CP, Warren GL, Armstrong RB. Intracellular Ca^{2+} transients in mouse soleus muscle after hindlimb unloading and reloading. J Appl Physiol 1999;87:386-390.

8. Mukhina AM, Altaeva EG, Nemirovskaya TL, Shenkman BS. The role of L-type calcium channels in the accumulation of Ca^{2+} in soleus muscle fibers in the rat and changes in the ratio of myosin and serca isoforms in conditions of gravitational unloading. Neurosci Behav Physiol 2008;38:181-188.

9. Zhu Y, Fan X, Li X, Wu S, Zhang H, Yu L. Effect of hindlimb unloading on resting intracellular calcium in intrafusal fibers and ramp-and-hold stretches evoked responsiveness of soleus muscle spindles in conscious rats. Neurosci Lett 2008;442:169-173.

10. Ingalls CP, Wenke JC, Armstrong RB. Time course changes in $[Ca^{2+}]_i$, force, and protein content in hindlimb-suspended mouse soleus muscles. Aviat Space Environ Med 2001;72:471-476.

11. Shenkman BS, Nemirovskaya TL. Calcium-dependent signaling mechanisms and soleus fiber remodeling under gravitational unloading. J Muscle Res Cell Motil 2008;29:221-230.

12. van der Velden JL, Langen RC, Kelders MC, Wouters EF, Janssen-Heininger YM, Schols AM. Inhibition of glycogen synthase kinase-3β activity is sufficient to stimulate myogenic differentiation. Am J Physiol Cell Physiol 2006;290:C453-462.

13. van der Velden JL, Langen RC, Kelders MC, Willems J, Wouters EF, Janssen-Heininger YM, et al. Myogenic differentiation during regrowth of atrophied skeletal muscle is associated with inactivation of GSK-3β. Am J Physiol Cell Physiol 2007;292:C1636-1644.

14. Friday BB, Horsley V, Pavlath GK. Calcineurin activity is required for the initiation of skeletal muscle differentiation. J Cell Biol 2000;149:657-666.

15. Przybylski RJ, MacBride RG, Kirby AC. Calcium regulation of skeletal myogenesis. I. Cell content critical to myotube formation. In Vitro Cell Dev Biol 1989;25:830-838.

16. Formigli L, Sassoli C, Squecco R, Bini F, Martinesi M, Chellini F, et al. Regulation of transient receptor potential canonical channel 1 (TRPC1) by sphingosine 1-phosphate in C2C12 myoblasts and its relevance for a role of mechanotransduction in skeletal muscle differentiation. J Cell Sci 2009;122:1322-1333.

17. Louis M, Zanou N, Van Schoor M, Gailly P. TRPC1 regulates skeletal myoblast migration and differentiation. J Cell Sci 2008;121:3951-3959.

18. Zanou N, Schakman O, Louis P, Ruegg UT, Dietrich A, Birnbaumer L, et al. TRPC1 ion channel modulates phosphatidylinositol 3-kinase/Akt pathway during myoblast differentiation and muscle regeneration. J Biol Chem 2012;287:14524-14534.

19. Clapham DE. TRP channels as cellular sensors. Nature 2003;426:517-524.

20. Vandebrouck C, Martin D, Colson-Van Schoor M, Debaix H, Gailly P. Involvement of TRPC in the abnormal calcium influx observed in dystrophic (*mdx*) mouse skeletal muscle fibers. J Cell Biol 2002;158:1089-1096.

21. Cheung KK, Yeung SS, Au SW, Lam LS, Dai ZQ, Li YH, et al. Expression and association of TRPC1 with TRPC3 during skeletal myogenesis. Muscle Nerve 2011;44:358-365.

22. Lee EH, Cherednichenko G, Pessah IN, Allen PD. Functional coupling between TRPC3 and RyR1 regulates the expressions of key triadic proteins. J Biol Chem 2006;281:10042-10048.

23. Rosenberg P, Hawkins A, Stiber J, Shelton JM, Hutcheson K, Bassel-Duby R, et al. TRPC3 channels confer cellular memory of recent neuromuscular activity. Proc Natl Acad Sci U S A 2004;101:9387-9392.

24. Zhang BT, Yeung SS, Liu Y, Wang HH, Wan YM, Ling SK, et al. The effects of low frequency electrical stimulation on satellite cell activity in rat skeletal muscle during hindlimb suspension. BMC Cell Biol 2010;11:87.

25. Zhang BT, Yeung SS, Allen DG, Qin L, Yeung EW. Role of the calcium-calpain pathway in cytoskeletal damage after eccentric contractions. J Appl Physiol 2008;105:352-357.

26. Livak KJ, Schmittgen TD. Analysis of relative gene expression data using real-time quantitative PCR and the 2(-Delta Delta C(T)) Method. Methods 2001;25:402-408.

27. Brinkmeier H. TRP channels in skeletal muscle: gene expression, function and implications for disease. Adv Exp Med Biol 2011;704:749-758.

28. Dumont N, Frenette J. Macrophages protect against muscle atrophy and promote muscle recovery in vivo and in vitro: a mechanism partly dependent on the insulin-like growth factor-1 signaling molecule. Am J Pathol 2010;176:2228-2235.

29. Washington TA, White JP, Davis JM, Wilson LB, Lowe LL, Sato S, et al. Skeletal muscle mass recovery from atrophy in IL-6 knockout mice. Acta Physiol (Oxf) 2011;202:657-669.

30. Itai Y, Kariya Y, Hoshino Y. Morphological changes in rat hindlimb muscle fibres during recovery from disuse atrophy. Acta Physiol Scand 2004;181:217-224.

31. Mitchell PO, Mills ST, Pavlath GK. Calcineurin differentially regulates maintenance and growth of phenotypically distinct muscles. Am J Physiol Cell Physiol 2002;282:C984-992.

32. Duan X, Berthiaume F, Yarmush D, Yarmush ML. Proteomic analysis of altered protein expression in skeletal muscle of rats in a hypermetabolic state induced by burn sepsis. Biochem J 2006;397:149-158.

33. Ambudkar IS, Ong HL, Liu X, Bandyopadhyay BC, Cheng KT. TRPC1: the link between functionally distinct store-operated calcium channels. Cell Calcium 2007;42:213-223.

34. Ohira T, Terada M, Kawano F, Nakai N, Ogura A, Ohira Y. Region-specific responses of adductor longus muscle to gravitational load-dependent activity in wistar hannover rats. PLoS One 2011;6:e21044.

35. Seo Y, Lee K, Park K, Bae K, Choi I. A proteomic assessment of muscle contractile alterations during unloading and reloading. J Biochem 2006;139:71-80.

36. Nagata Y, Partridge TA, Matsuda R, Zammit PS. Entry of muscle satellite cells into the cell cycle requires sphingolipid signaling. J Cell Biol 2006;174:245-253.

37. Zeidan YH, Hannun YA. Translational aspects of sphingolipid metabolism. Trends Mol Med 2007;13:327-336.

38. Olah T, Fodor J, Ruzsnavszky O, Vincze J, Berbey C, Allard B, et al. Overexpression of transient receptor potential canonical type 1 (TRPC1) alters both store operated calcium entry and depolarization-evoked calcium signals in C2C12 cells. Cell Calcium 2011;49:415-425.

39. Guo BS, Cheung KK, Yeung SS, Zhang BT, Yeung EW. Electrical stimulation influences satellite cell proliferation and apoptosis in unloading-induced muscle atrophy in mice. PLoS One 2012;7:e30348.

40. Kawano F, Takeno Y, Nakai N, Higo Y, Terada M, Ohira T, et al. Essential role of satellite cells in the growth of rat soleus muscle fibers. Am J Physiol Cell Physiol 2008;295:C458-467.

41. Wang XD, Kawano F, Matsuoka Y, Fukunaga K, Terada M, Sudoh M, et al. Mechanical load-dependent regulation of satellite cell and fiber size in rat soleus muscle. Am J Physiol Cell Physiol 2006;290:C981-989.

42. Kasper CE, Xun L. Expression of titin in skeletal muscle varies with hind-limb unloading. Biol Res Nurs 2000;2:107-115.

43. Shenkman BS, Nemirovskaya TL, Belozerova IN, Vikhlyantsev IM, Matveeva OA, Staroverova KS, et al. Effects of Ca^{2+}-binding agent on unloaded rat soleus: muscle morphology and sarcomeric titin content. J Gravit Physiol 2002;9:P139-140.

44. Jackman RW, Kandarian SC. The molecular basis of skeletal muscle atrophy. Am J Physiol Cell Physiol 2004;287:C834-843.

45. Kandarian SC, Jackman RW. Intracellular signaling during skeletal muscle atrophy. Muscle Nerve 2006;33:155-165.

46. Singh BB, Liu X, Tang J, Zhu MX, Ambudkar IS. Calmodulin regulates Ca^{2+}-dependent feedback inhibition of store-operated Ca^{2+} influx by interaction with a site in the C terminus of TrpC1. Mol Cell 2002;9:739-750.

47. Beech DJ, Xu SZ, McHugh D, Flemming R. TRPC1 store-operated cationic channel subunit. Cell Calcium 2003;33:433-440.

48. Sugiura T, Abe N, Nagano M, Goto K, Sakuma K, Naito H, et al. Changes in PKB/Akt and calcineurin signaling during recovery in atrophied soleus muscle induced by unloading. Am J Physiol Regul Integr Comp Physiol 2005;288:R1273-1278.

49. Oishi Y, Ogata T, Yamamoto KI, Terada M, Ohira T, Ohira Y, et al. Cellular adaptations in soleus muscle during recovery after hindlimb unloading. Acta Physiol (Oxf) 2008;192:381-395.

50. Pigozzi D, Ducret T, Tajeddine N, Gala JL, Tombal B, Gailly P. Calcium store contents control the expression of TRPC1, TRPC3 and TRPV6 proteins in LNCaP prostate cancer cell line. Cell Calcium 2006;39:401-415.

51. Xi Q, Adebiyi A, Zhao G, Chapman KE, Waters CM, Hassid A, et al. IP3 constricts cerebral arteries via IP3 receptor-mediated TRPC3 channel activation and independently of sarcoplasmic reticulum Ca^{2+} release. Circ Res 2008;102:1118-1126.

52. Kuwahara K, Wang Y, McAnally J, Richardson JA, Bassel-Duby R, Hill JA, et al. TRPC6 fulfills a calcineurin signaling circuit during pathologic cardiac remodeling. J Clin Invest 2006;116:3114-3126.

Table 1.

	Body Weight (g)	
	Experimental Group	**Age-matched Control Group**
7U	21.37 ± 0.51	22.85 ± 0.36
14U	22.95 ± 1.16	24.18 ± 0.82
3R	23.19 ± 0.11	24.90 ± 0.72
7R	22.28 ± 0.68	23.75 ± 0.60
14R	25.85 ± 0.95	26.01 ± 0.93
28R	25.05 ± 0.58	26.70 ± 1.02

TABLE LEGENDS

Table 1. Body weight for each experimental group: 7 or 14 days of unloading (7U or 14U); 3, 7, 14, and 28 days of reloading (3R, 7R, 14R, 28R). Age-matched controls were compared at termination of experiments. Values are means ± SEM; $n = 5$ for each group.

FIGURE LEGENDS

FIGURE 1. Soleus muscle mass changes during unloading and reloading. Soleus muscle mass normalized to body weight after 7 or 14 days of unloading (7U or 14U), followed by 3, 7, and 14 days of reloading (3R, 7R, 14R). Control, age-matched, weight-bearing controls; Experimental, unloading and reloading groups; $n = 5$. Values are means ± SEM. $^{*}P < 0.05$, $^{**}P < 0.01$ compared to controls, $^{\#}P < 0.01$ in comparison with 14U experimental group.

FIGURE 2. Changes in muscle fiber cross-sectional area during unloading and reloading. Soleus muscle fiber cross sectional area (CSA) after 7 or 14 days of unloading (7U or 14U), followed by 3, 7, 14, and 28 days of reloading (3R, 7R, 14R, 28R). Control: age-matched, weight-bearing controls; Experimental: unloading and reloading groups; $n = 5$. Values are means ± SEM. $^{*}P < 0.05$, $^{**}P < 0.01$ in comparison with controls; $^{\#}P < 0.05$, $^{\#\#\#}P < 0.001$ in comparison with 14U experimental group.

FIGURE 3. Changes in peak tetanic force during unloading and reloading. Peak tetanic force (P_o) normalized to soleus muscle cross sectional area after 7 or 14 days of unloading (7U or 14U), followed by 3, 7, and 14 days of reloading (3R, 7R, 14R). Control: age-matched, weight-bearing controls; Experimental: unloading and reloading groups; $n = 5$. Values are means ± SEM. $^{*}P < 0.05$, $^{**}P < 0.01$ in comparison to controls, $^{\#\#}P < 0.01$ in comparison with 7U, 14U and 3R experimental groups.

FIGURE 4. mRNA expression of TRPC1 and TRPC3. (**A**) mRNA expression of TRPC1 and (**B**)TRPC3 after 7 or 14 days of unloading (7U or 14U), followed by 3, 7, and 14 days of reloading (3R, 7R, 14R). CON: control, $n = 5$. Values are means ± SEM. $^{*}P < 0.05$ in comparison with control; $^{\#}P < 0.05$, $^{\#\#}P < 0.01$ in comparison with 14R.

FIGURE 5. Western blot expression of TRPC1 and TRPC3. (**A**) Western blot analysis of TRPC1 and (**B**) TRPC3 in soleus muscle after 7 or 14 days of unloading (7U or 14U), followed by 3, 7, 14, and 28 days of reloading (3R, 7R, 14R, 28R). CON: control. Data were quantified by normalizing the band intensity of TRPC to GAPDH and were expressed as the percentage of age-matched, weight-bearing controls. Values are means ± SEM. $*P < 0.05$; $**P < 0.01$; $***P < 0.001$ in comparison with controls; $^{###}P < 0.001$ in comparison with 28R.

FIGURE 6. Immunostaining images for TRPC1 and TRPC3. (**A**) Representative cross-sectional images of soleus muscle immunostained for TRPC1 expression (green) after 14 days unloading (14U) followed by 14 and 28 days of reloading (14R, 28R). Counterstaining was performed with TRITC-conjugated WGA to label plasma membrane (red). Yellow color in the merged images indicates co-localization. (**B**) Representative images of TRPC3 expression (green) after 14 days unloading (14U) followed by 7 and 14 days of reloading (7R, 14R). Scale bar = 50 μm.

Figure 1.

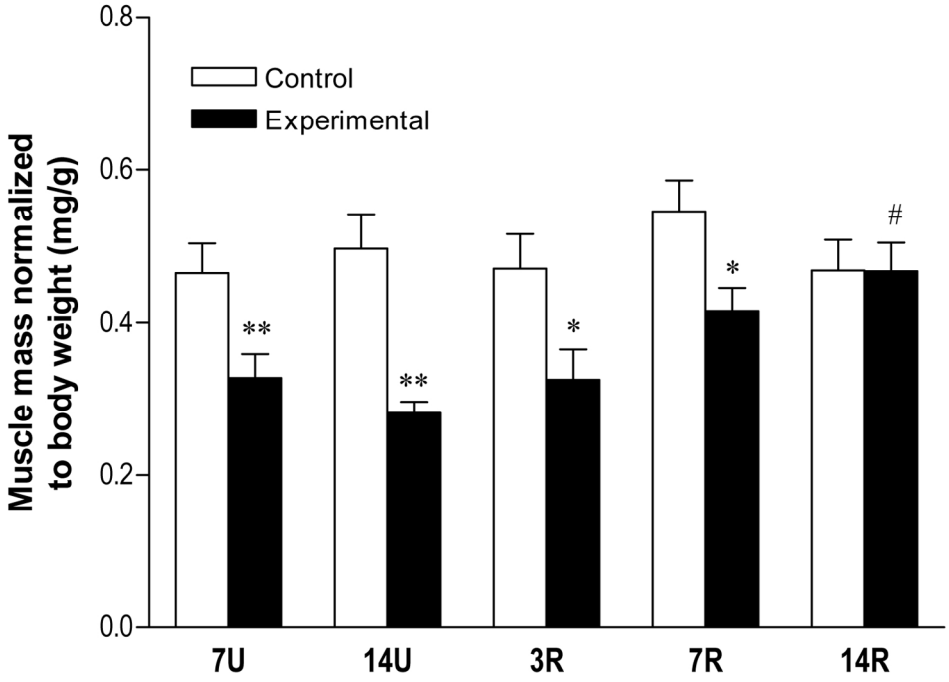

Soleus muscle mass changes during unloading and reloading. Soleus muscle mass normalized to body weight after 7 or 14 days of unloading (7U or 14U), followed by 3, 7, and 14 days of reloading (3R, 7R, 14R). Control, age-matched, weight-bearing controls; Experimental, unloading and reloading groups; n = 5. Values are means ± SEM. * $P < 0.05$, ** $P < 0.01$ compared to controls, # $P < 0.01$ in comparison with 14U experimental group.
140x122mm (300 x 300 DPI)

Figure 2.

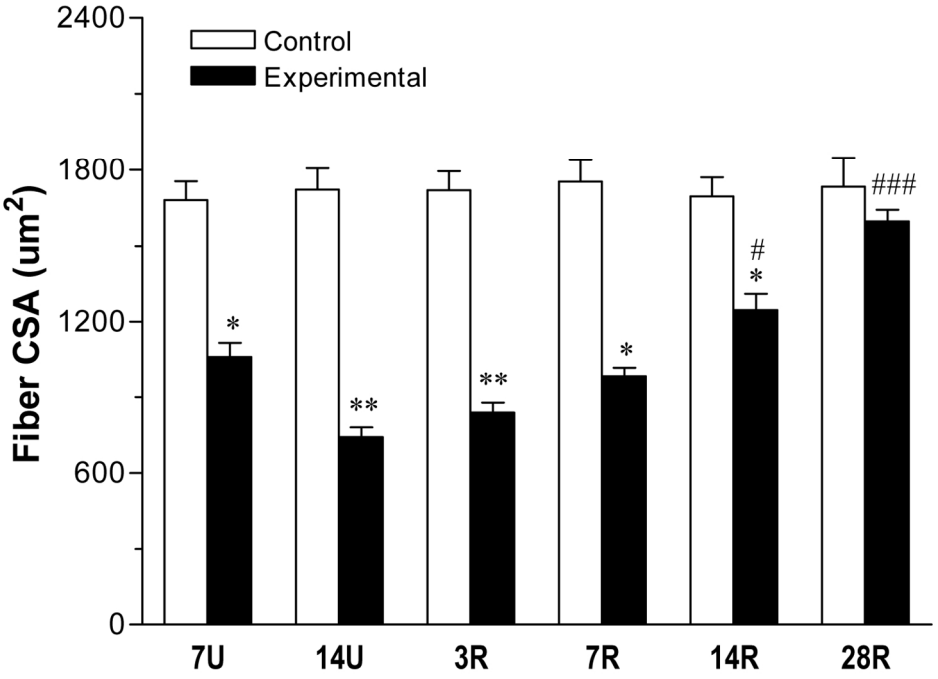

Changes in muscle fiber cross-sectional area during unloading and reloading. Soleus muscle fiber cross sectional area (CSA) after 7 or 14 days of unloading (7U or 14U), followed by 3, 7, 14, and 28 days of reloading (3R, 7R, 14R, 28R). Control, age-matched, weight-bearing controls; Experimental, unloading and reloading groups; n = 5. Values are means ± SEM. *P < 0.05, **P < 0.01 in comparison with controls; #P < 0.05, ###P < 0.001 in comparison with 14U experimental group.
138x117mm (300 x 300 DPI)

Figure 3.

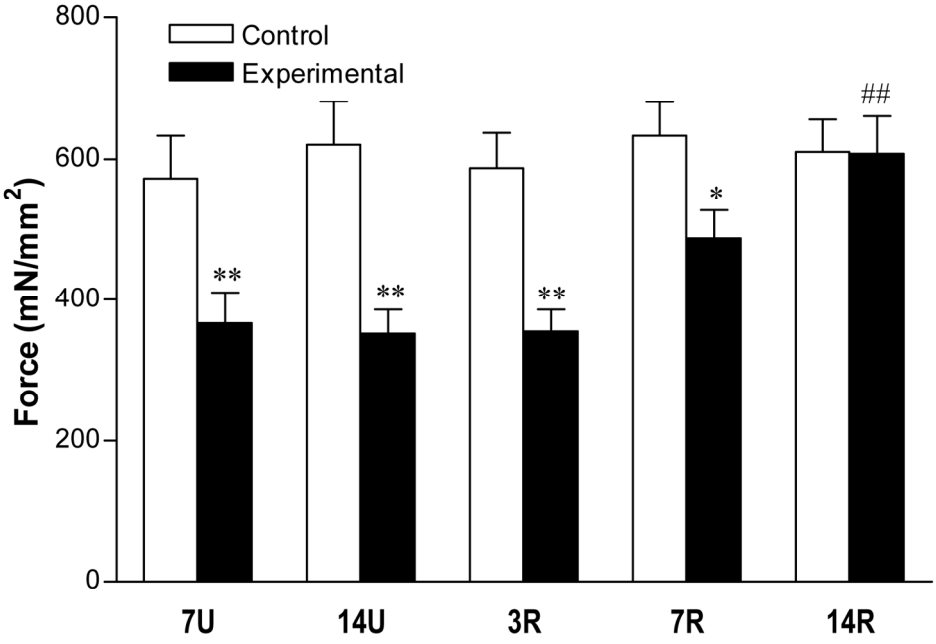

Changes in peak tetanic force during unloading and reloading. Peak tetanic force (Po) normalized to soleus muscle cross sectional area after 7 or 14 days of unloading (7U or 14U), followed by 3, 7, and 14 days of reloading (3R, 7R, 14R). Control, age-matched, weight-bearing controls; Experimental, unloading and reloading groups; n = 5. Values are means ± SEM. *P < 0.05, **P < 0.01 in comparison to controls, ##P < 0.01 in comparison with 7U, 14U and 3R experimental groups.
148x130mm (300 x 300 DPI)

Figure 4.

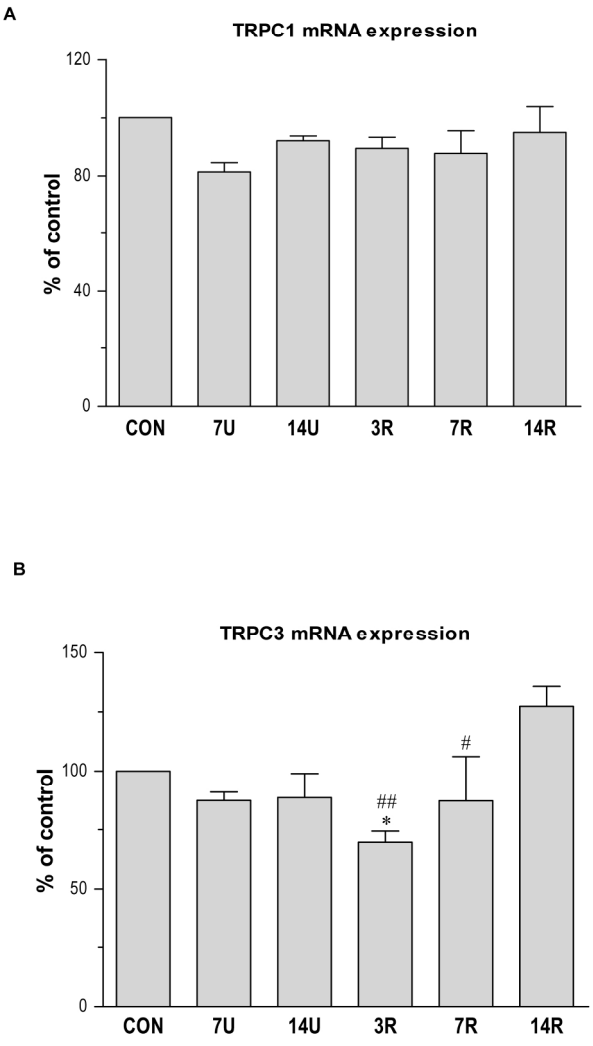

mRNA expression of TRPC1 and TRPC3. (A) mRNA expression of TRPC1 and (B)TRPC3 after 7 or 14 days of unloading (7U or 14U), followed by 3, 7, and 14 days of reloading (3R, 7R, 14R). CON, control. n = 5. Values are means ± SEM. *P < 0.05 in comparison with control; #P < 0.05, ##P < 0.01 in comparison with 14R.
136x240mm (300 x 300 DPI)

Figure 5.

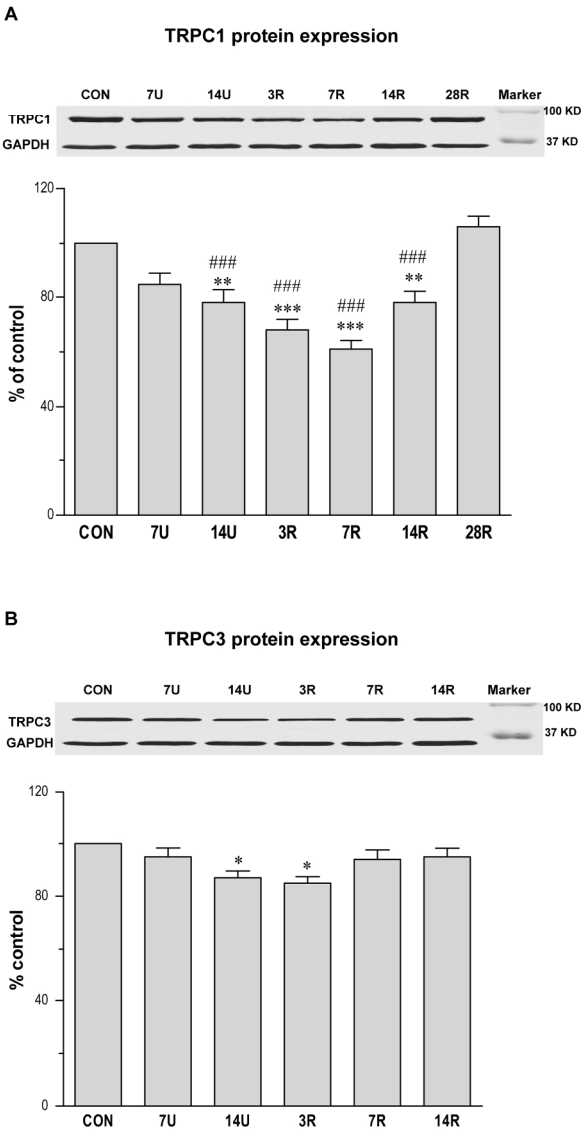

Western blot expression of TRPC1 and TRPC3. (A) Western blot analysis of TRPC1 and (B) TRPC3 in soleus muscle after 7 or 14 days of unloading (7U or 14U), followed by 3, 7, 14, and 28 days of reloading (3R, 7R, 14R, 28R). CON: control. Data were quantified by normalizing the band intensity of TRPC to GAPDH and were expressed as the percentage of age-matched, weight-bearing controls. Values are means ± SEM. *P < 0.05; **P < 0.01; ***P < 0.001 in comparison with controls; ###P < 0.001 in comparison with 28R.
111x225mm (300 x 300 DPI)

Figure 6.

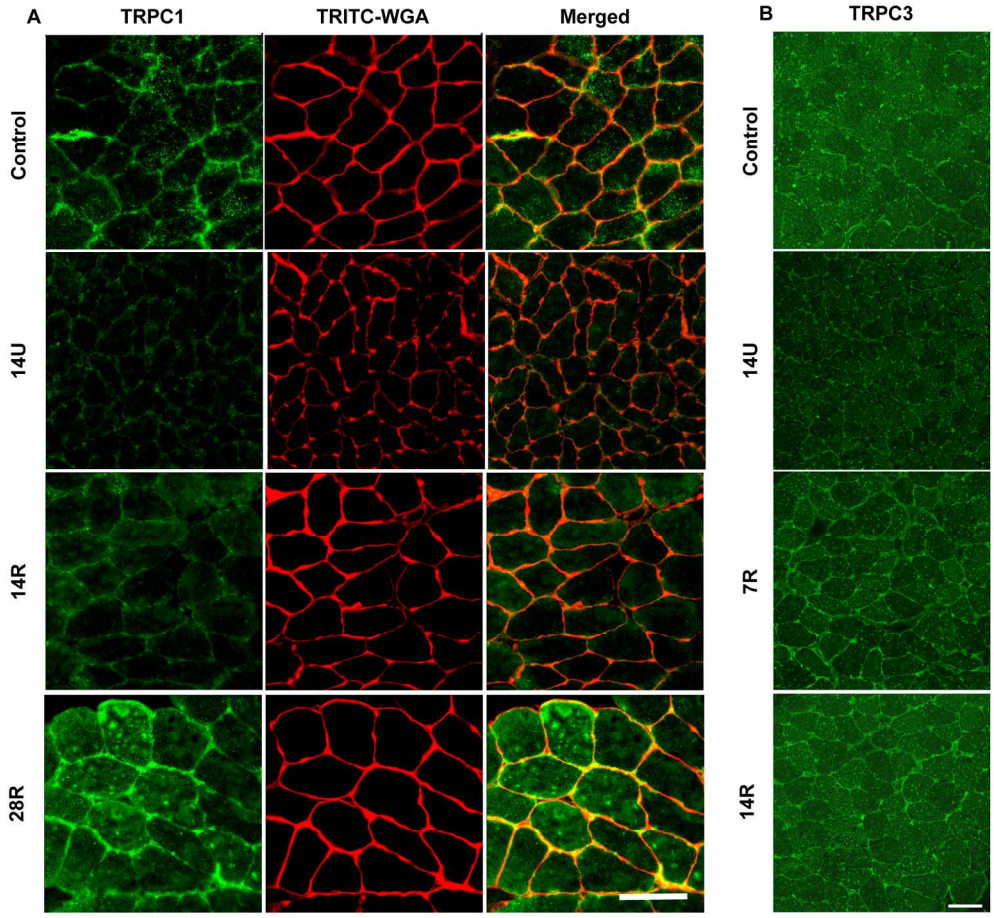

Immunostaining images for TRPC1 and TRPC3. (A) Representative cross-sectional images of soleus muscle immunostained for TRPC1 expression (green) after 14 days unloading (14U) followed by 14 and 28 days of reloading (14R, 28R). Counterstaining was performed with TRITC-conjugated WGA to label plasma membrane (red). Yellow color in the merged images indicates co-localization. (B) Representative images of TRPC3 expression (green) after 14 days unloading (14U) followed by 7 and 14 days of reloading (7R, 14R). Scale bar = 50 μm.
179x175mm (300 x 300 DPI)